DIVISION S-1—SOIL PHYSICS

Relationship between the Hydraulic Conductivity Function and the Particle-Size Distribution

Lalit M. Arya,* Feike J. Leij, Peter J. Shouse, and Martinus Th. van Genuchten

ABSTRACT

We present a model to compute the hydraulic conductivity, K, as a function of water content, θ, directly from the particle-size distribution (PSD) of a soil. The model is based on the assumption that soil pores can be represented by equivalent capillary tubes and that the water flow rate is a function of pore size. The pore-size distribution is derived from the PSD using the Arya-Paris model. Particle-size distribution and $K(\theta)$ data for 16 soils, representing several textural classes, were used to relate the pore flow rate and the pore radius according to $q_i = cr_i^x$, where q_i is the pore flow rate ($cm^3\ s^{-1}$) and r_i is the pore radius (cm). Log c varied from about -2.43 to about 2.78, and x varied from ≈ 2.66 to ≈ 4.71. However, these parameters did not exhibit a systematic trend with textural class. The model was used to independently compute the $K(\theta)$ function, from the PSD data for 16 additional soils. The model predicted $K(\theta)$ values from near saturation to very low water contents. The agreement between the predicted and experimental $K(\theta)$ for individual samples ranged from excellent to poor, with the root mean square residuals (RMSR) of the log-transformed $K(\theta)$ ranging from 0.616 to 1.603 for sand, from 0.592 to 1.719 for loam, and from 0.487 to 1.065 for clay. The average RMSR for all textures was 0.878.

KNOWLEDGE OF THE HYDRAULIC CONDUCTIVITY as a function of water content, $K(\theta)$, or pressure head, $K(h)$, is essential for many problems involving water flow and mass transport in unsaturated soils. A variety of field and laboratory techniques have been developed to directly measure the unsaturated hydraulic conductivity (e.g., Klute and Dirksen, 1986; Green et al., 1986; Dirksen, 1991). While research continues to improve physical measurements of flow parameters and analytical techniques (e.g., Smettem and Clothier, 1989; Eching et al., 1994; Wildenschild et al., 1997), it is unlikely that one standard methodology will become available that is satisfactory for all applications. Hence, considerable efforts have been devoted to the indirect estimation of the hydraulic conductivity function (e.g., van Genuchten and Leij, 1992; Mualem, 1992). These efforts are justified, since direct measurements of the hydraulic properties are costly and time consuming and the results are variable, error-prone, and applicable to only a narrow range of saturation. Additionally, the number of measurements required to adequately characterize K in the field is prohibitive given the natural soil variability.

Estimation of the hydraulic conductivity function is typically based on models that consider the pore-size distribution of a soil (e.g., Childs and Collis-George, 1950; Marshall, 1958; Mualem, 1976; van Genuchten, 1980). Input data for these types of models generally include a measured or estimated soil water retention function, $h(\theta)$, and the saturated conductivity, K_s. The hydraulic conductivity is derived by integration of elementary pore domains, represented by a specific pore radius. The range of the predicted $K(\theta)$ function is generally limited to the saturation range for which $h(\theta)$ data are available. A more generalized formulation includes pore tortuosity, pore connectivity, or pore interaction terms (e.g., Mualem and Dagan, 1978). However, since geometric descriptions of these parameters are not available, they are evaluated empirically from more easily measured soils data such as soil texture, bulk density, and organic matter content (e.g., Schuh and Bauder, 1986; Wösten and van Genuchten, 1988; Vereecken et al., 1990; Vereecken, 1995). Model parameters are often expressed as averages for the different textural classes, with considerable uncertainty in predicted $K(\theta)$ functions. The problem is compounded as the number of parameters increases, especially if $h(\theta)$ input data are also based on a model (e.g., Wösten and van Genuchten, 1988; Vereecken, 1995). Thus, there is a need for models that accurately reflect phenomenological properties of observed hydraulic conductivity functions, but that contain as few unknown parameters as possible (e.g., van Genuchten and Leij, 1992; Poulsen et al., 1998).

The utility of pore-size distribution models to predict the hydraulic conductivity function, $K(\theta)$, from the water retention characteristic, $h(\theta)$, and the saturated hydraulic conductivity, K_s, implies that $K(\theta)$ can be related to the same basic soil properties that are commonly used to characterize $h(\theta)$ and K_s. This may be accomplished with so-called pedotransfer functions that empirically predict hydraulic properties from basic soil properties (e.g., Bouma and van Lanen, 1987; van Genuchten and Leij, 1992). However, soil properties seldom, if ever, directly constitute formative elements of the models. Commonly available models are mathematical descriptions of the shapes of $h(\theta)$ and $K(\theta)$ curves with unknown parameters. Much of the effort appears to have been focused on relating parameters of mathematical functions to basic soil properties (e.g., Schuh and Bauder, 1986; Wösten and van Genuchten, 1988; Schuh and Cline, 1990; Vereecken et al., 1990; Vereecken, 1995).

Basic soil properties such as PSD and bulk density

US Salinity Lab., USDA-ARS, 450 W. Big Springs Rd., Riverside, CA 92507. Received 2 Oct. 1998. *Corresponding author (larya@ussl.ars.usda.gov).

Published in Soil Sci. Soc. Am. J. 63:1063–1070 (1999).

Abbreviations: PSD, particle-size distribution; RMSR, root mean square residuals.

are widely available for many soil types and can be accurately and routinely determined in laboratories around the world. Hence, formulation of hydraulic properties entirely in terms of basic soil properties should be of considerable benefit. Translation of the PSD into a corresponding water retention function has been accomplished using the concept that the pore-size distribution is directly related to PSD (e.g., Arya and Paris, 1981; Tyler and Wheatcraft, 1988; Rieu and Sposito, 1991; Arya et al., 1999). In view of the above, it is possible to also quantitatively relate the hydraulic conductivity of a soil to its PSD. The objective of this research was to formulate a relationship between the hydraulic conductivity function and the PSD, and to evaluate predictions of the conductivity obtained by this relationship.

MODEL DEVELOPMENT

Following Hagen-Poiseuille's equation and following other studies in soil hydraulics, we base this model on the premise that flow in soil pores is a function of the pore radius, with pore radii determined by the PSD. Additionally, we assume that the hydraulic conductivity of a soil, at a given saturation, is made up of contributions from flow in pores that remain completely filled with water at that saturation; that is, the contribution of partially drained pores to overall flow is insignificant. Although these are simplified assumptions, they help to formulate a model of flow which can be calibrated for more complex media.

Based on the above simplifications, the hydraulic conductivity of a soil with its pore volume divided into n pore-size fractions, and with fractions 1 through i filled with water, can be expressed according to Darcy's law as

$$K(\theta_i) = \frac{L}{A\,\Delta H}\sum_{j=1}^{j=i} Q_j; \qquad i = 1, 2, ..., n \qquad [1]$$

where $K(\theta_i)$ is the hydraulic conductivity of the sample (cm s^{-1}) corresponding with water content θ_i ($cm^3\ cm^{-3}$), L is the sample length (cm), ΔH is the hydraulic head difference (cm) across the sample length in the direction of flow, A is the cross-sectional area of the sample (cm^2), and Q_j is the volumetric outflow rate ($cm^3\ s^{-1}$) contributed by the jth pore fraction. A complete list of variables used in the equations is provided in Table 1.

The water content, θ_i, can be calculated from PSD, porosity, and maximum measured water content information, according to

$$\theta_i = (\phi S_w)\sum_{j=1}^{j=i} w_j; \qquad i = 1, 2, ..., n \qquad [2]$$

where ϕ is the total porosity ($cm^3\ cm^{-3}$), S_w is the ratio of measured saturated water content to total porosity, and w_j is the mass fraction of particles (g) in the jth particle-size fraction. To compute water content, the PSD is divided into n fractions, and the difference in cumulative percentages corresponding with successive particle sizes is divided by 100 to obtain values of w_j such that the sum of all w_j is unity. The pore volume associated with the solid mass in each fraction is calculated on the basis of the assumption that the bulk and particle densities of the bulk sample apply to each fraction. The volumetric water content is given by a summation of the individual pore volumes (from fraction j = 1 to fraction $j = i$) divided by the bulk volume of the sample. Further information on scaling water content from the PSD can be found in Arya and Paris (1981) and Arya et al. (1999). The value of S_w normally varies from 0.85 to 0.95 for nonswelling soils. For soils with high clay content, S_w may be progressively modified with changes in sample volume that accompany wetting and drying (e.g., Garnier et al., 1997).

The volumetric flow rate, Q_i, can be written as the sum of the flow rates of individual saturated pores within the ith pore fraction of a particular soil sample. Thus,

$$Q_i = q_i N_{pi} \qquad [3]$$

where q_i is the volumetric flow rate for a single pore ($cm^3\ s^{-1}$) and N_{pi} is the number of pores in the ith pore-size fraction.

Table 1. Variables used in the equations.

Variable	Description	Dimension†
A	cross-sectional area, bulk sample	L_b^2
a	pore cross-section, single pore	L_p^2
e	void ratio $(\rho_s - \rho_b)/\rho_b$	$L_p^3 L_s^{-3}$
H	hydraulic head	L_w
K	hydraulic conductivity	$L_w T^{-1}$
L	flow path length	L_w
n_i	number of spherical particles, ith fraction	–
N_i	scaled number of spherical particles, ith fraction	–
N_{pi}	number of pores, ith fraction	–
Q_i	volumetric flow rate, ith pore fraction	$L_w^3\ T^{-1}$
q_i	volumetric flow rate for a single pore, ith pore fraction	$L_w^3\ T^{-1}$
r_i	mean pore radius, ith fraction	L_p
R_i	mean particle radius, ith fraction	L_s
S	shape factor	–
S_w	ratio of maximum water content to porosity	–
w_i	mass fraction, solid particles, ith fraction	M_s^{-1}
x	exponent on pore radius	–
α	scaling parameter	–
η	viscosity of water	$M_w\ L^{-1}\ T^{-1}$
θ_i	volumetric water content, ith fraction	$L_w^3\ L_b^{-3}$
ρ_b	bulk density	$M_s\ L_b^{-3}$
ρ_s	particle density	$M_s\ L_s^{-3}$
ϕ	porosity	$L_p^3\ L_b^{-3}$

† For dimensional analysis, L = length, M = mass, and T = time, with subscripts b for bulk, e for effective, m for measured, p for pore, s for solid and saturated, and w for water.

Flow in a Single Pore

Flow at the microscopic pore scale cannot be precisely defined. We conceptualize an individual pore as an equivalent capillary tube in which flow occurs according to the Hagen-Poiseuille law for capillary flow (e.g., Batchelor, 1967; Hillel, 1971). The flow rate, q_i, for an individual pore can be calculated from

$$q_i = \frac{\pi r_i^x}{S\eta}\frac{\rho_w g \Delta H}{L} \qquad [4]$$

where r_i is the mean pore radius (cm) for the ith pore fraction, ρ_w is the density of water (g cm^{-3}), g is the acceleration due to gravity (cm s^{-2}), ΔH is the pressure head difference across the flow path (cm), S is a shape

factor, η is the viscosity of water (g cm^{-1} s^{-1}), and L is the length of the flow path (cm). The term $(\Delta H/L)$ in Eq. [4] can be eliminated if flow occurs under a unit gradient. The exponent x and the shape factor S are dimensionless parameters. For cylindrical tubes of uniform diameter, $x = 4$ and $S = 8$.

Soil pores, however are neither circular nor uniform. Nor are they straight. Therefore, an adjustment of parameters S and x is necessary to adapt Eq. [4] for natural materials. Flow of water in soil pores is affected by a number of factors, including pore size, the spatial and relative distribution of pores of various sizes, pore shape, tortuosity, pore connectivity, fluid properties, and as the degree of saturation (e.g., Mualem, 1992; Corey, 1992). However, it is intuitive from the Hagen-Poiseuille equation and other studies in soil hydraulics (e.g., Childs, 1969) that pore size should have an overwhelming effect on flow rate. While factors such as pore shape and tortuosity are important, a satisfactory geometric description of these factors is as yet unavailable. Therefore, we follow a pragmatic approach, assume a unit gradient, and combine all factors except for pore size in a single empirical variable. As a result, Eq. [4] is modified to

$$q_i = cr_i^x \qquad [5]$$

in which c and x can be evaluated empirically using experimental data.

The Pore Radius, r_i

The pore radius, r_i, can be calculated from the PSD according to Arya and Paris (1981), using

$$r_i = 0.816R_i\sqrt{en_i^{(1-\alpha i)}} \qquad [6]$$

where R_i is the mean particle radius for the ith particle-size fraction, e is the void ratio of the natural-structured soil sample, n_i is the number of equivalent spherical particles in the fraction, and α_i is the scaling parameter defined by Arya et al. (1999) as

$$\alpha_i = \log N_i/\log n_i \qquad [7]$$

where N_i represents the scaled number of hypothetical spherical particles of radius R_i required to trace the tortuous pore length contributed by n_i natural particles in the actual sample. Note that the terms e and $n_i^{(1-\alpha_i)}$ in Eq. [6] are dimensionless. The equivalent number of spherical particles, n_i in the ith particle-size fraction can be calculated from

$$n_i = 3w_i/4\pi\rho_s R_i^3 \qquad [8]$$

The void ratio, e is given by

$$e = (\rho_s - \rho_b)/\rho_b \qquad [9]$$

where ρ_s is the particle density (g cm^{-3}) and ρ_b is the bulk density (g cm^{-3}) of the natural-structured (undisturbed) sample.

The scaled number of spherical particles, N_i can be obtained from the PSD using the empirical relationship (Arya et al., 1999):

$$\log N_i = a + b\log(w_i/R_i^3) \qquad [10]$$

Table 2. Parameters of Eq. [10] relating log N_i to log(w_i/R_i^3), and the goodness of fit, r^2, for four soil textural classes.†

Textural class	Soils	Data pairs	a	b	r^2
Sand	6	62	−2.478	1.490	0.882
Sandy loam	6	75	−3.398	1.773	0.952
Loam	4	50	−1.681	1.395	0.936
Clay	5	88	−2.600	1.305	0.954

† cf. Arya et al., 1999.

Table 2 summarizes parameters a and b and the goodness of fit, r^2, for four soil textures included in the study of Arya et al. (1999). Particle-size distribution, bulk density, and soil water characteristic data to establish Eq. [10] for the soils in Table 2 were obtained from the UNSODA soil hydraulic properties database (Leij et al., 1996). Once Eq. [10] is specified, there is no need to know the water retention characteristic, $h(\theta)$.

Number of Pores, N_{pi}

We assume that ratio of the total pore area exposed at the cross-sectional area of a sample is the same as effective porosity of the sample. Thus, for a natural-structure sample of unit mass

$$A_{pe} = \phi_e A_b \qquad [11]$$

where A_{pe} is the total effective pore area exposed at the sample cross section, ϕ_e is the effective porosity given by $\phi_e = S_w\,[1 - (\rho_b/\rho_s)]$, and A_b is the cross-sectional area of the sample given by $A_b = (1/\rho_b)^{2/3}$. Following Arya and Paris (1981), we distribute the effective pore area among the various pore-size fractions according to solid mass, w_i, in the various particle-size fractions, that is,

$$A_{pi} = A_{pe}w_i \qquad [12]$$

where A_{pi} is the effective pore area attributed to the ith pore-size fraction. The number of pores in the ith pore fraction, N_{pi}, exposed at the cross-sectional area, can be obtained by dividing A_{pi} by the cross-sectional area of a single pore, a_{pi}. Thus,

$$N_{pi} = A_{pi}/a_{pi} \qquad [13]$$

where $a_{pi} = \pi r_i^2$ and r_i can be determined from PSD data according to Eq. [6].

The Hydraulic Conductivity Function, $K(\theta_i)$

For flow under a unit gradient, Eq. [1], [3], and [5] can be combined to formulate the $K(\theta_i)$ function as

$$K(\theta_i) = \frac{1}{A_b}\sum_{j=1}^{j=i}(cr_j^x)\,N_{pj}; \qquad i = 1, 2, ..., n \qquad [14]$$

Substitution for r_j (Eq. [6]) and N_{pj} (Eq. [11], [12], [13]) results in Eq. [15], which describes $K(\theta_i)$ expressly in terms of parameters of the PSD and packing characteristics of the sample.

$$K(\theta_i) = \frac{c\phi_e}{\pi}\sum_{j=1}^{j=i} R_j^{(x-2)}w_j\,[0.667en_j^{(1-\alpha j)}]^{(x-2)/2}; \qquad i = 1, 2, ..., n \qquad [15]$$

The summation in Eq. [14] and [15] for $i = n$ leads to the value of the saturated conductivity, K_s.

MATERIALS AND METHODS

Soils data used in this study were taken from the UNSODA hydraulic properties database (Leij et al., 1996). The parameters c and x were calibrated by fitting experimental conductivity data to the flow model given by Eq. [5]. The parameters were determined for sand, sandy loam, loam, and clay textures. Within each textural class, three or four data sets were used to evaluate c and x. In the second part of this study, the empirical values of c and x were used to independently predict $K(\theta)$ functions from PSD data for different data sets. Gross textural characteristics and bulk density data for soils used in this study are given in Table 3.

Evaluation of Parameters c and x

First, the cumulative PSD curve for the soil was converted into a corresponding pore-size vs. water content curve on the basis of procedures initially proposed by Arya and Paris (1981) and later refined by Arya et al. (1999). Measured values of the hydraulic conductivity, $K(\theta_i)_m$, corresponding with calculated water contents, were interpolated from plots of the experimental $K(\theta)$ curves. Since each calculated water content corresponded with a pore radius, it was possible to generate $K(\theta_i)_m$ vs. r_i pairs across a range of water contents. Backward calculations were then performed to obtain estimates of the measured values of the pore flow rates, $(q_i)_m$, corresponding with the pore sizes with which $K(\theta i)_m$ values were paired. It follows from Eq. [1] that multiplying $K(\theta i)_m$ by the cross-sectional area of the sample yields the total flow for the sample per unit time and per unit gradient. This flow volume represents the sum of flow volumes being contributed by all pore fractions that remain filled at the water content, $(\theta i)_m$. Thus,

$$A_b K(\theta_i)_m = \sum_{j=1}^{j=i} (Q_j)_m; \qquad i = 1, 2, ..., n \qquad [16]$$

and

$$(Q_i)_m = A_b[K(\theta_i)_m - K(\theta_{i-1})_m] \qquad [17]$$

where $(Q_i)_m$ is an estimate of the experimental volumetric flow rate for the ith pore fraction. An approximation of the measured flow rate for a single pore, $(q_i)_m$, in the ith pore fraction can be obtained from

$$(q_i)_m = (Q_i)_m/N_{p_i} \qquad [18]$$

Replacing q_i in Eq. [5] by $(q_i)_m$ and rewriting the equation in logarithmic form, we have

$$\log(q_i)_m = \log c + x \log r_i \qquad [19]$$

The parameters c and x were evaluated from plots of log $(q_i)_m$ vs. log r_i data. The UNSODA data sets used in this study and the values of log c and x along with goodness of fit, r^2, are presented in Table 3.

Calculation of Hydraulic Conductivity Function, $K(\theta_i)$

The PSD is divided into n particle-size fractions (usually 20 or more uniformly spaced increments of logarithm of the particle size) to yield n corresponding pairs of mass fraction, w_i, and mean particle radii, R_i. Each w_i is converted to an equivalent number of spherical particles, n_i, using Eq. [8]. The scaled number of spherical particles, N_i, is calculated for each fraction using Eq. [10] and Table 2. Particle numbers obtained from Eq. [8] and [10] are used in Eq. [7] to calculate the scaling parameter, α_i for each particle-size fraction. Mean R_i, n_i, and α_i for each fraction and the void ratio, e, for the natural soil sample (Eq. [9]) are used in Eq. [6] to compute mean pore radii, r_i. Values of water content, θ_i, are obtained by summing the pore volumes from fraction $j = 1$ to i, adjusting

Table 3. UNSODA soils used for model calibration and testing, model parameters log c and x in Eq. [19], goodness of fit, r^2, shape factor log S, and root mean square residuals (RMSR) of log-transformed $K(\theta)_{calc.}$ and $K(\theta)_{mean}$ data.

	Model calibration								Model test				
Texture	Code†	Clay	Sand	ρ_b	log c	x	r^2	log S	Code†	Clay	Sand	ρ_b	RMSR
		— % —		g cm^{-3}						— % —		g cm^{-3}	
Sand	1050	3.2	92.2	1.600	2.590	4.714	0.978	2.949	4000	1.5	93.8	1.460	0.669
	4650	1.0	94.0	1.622	2.507	4.471	0.970	3.032	1063	4.0	93.0	1.550	0.638
	4661	3.0	92.9	1.490	2.226	4.095	0.883	3.313	1043	3.0	93.0	1.593	1.603
	1464	2.4	93.0	1.67	0.171	2.808	0.963	5.368	4171	11.7	65.1	1.480	0.616
	1061	4.0	91.0	1.590	1.642	3.718	0.916	3.897	1054	2.5	97.2	1.540	1.563
Average					1.849	3.999	0.913	3.690					1.000
Sandy loam	1381	11.0	61.2	1.730	−0.952	3.000	0.977	6.491					
	1130	7.0	71.0	1.560	−0.808	2.882	0.981	6.347					
	4160	11.2	66.3	1.700	−2.426	2.664	0.972	7.965					
	4162	19.4	65.0	1.520	0.231	3.351	0.987	5.308					
Average					−0.871	3.063	0.964	6.410					
Loam	3192	16.3	44.2	1.440	2.392	4.139	0.996	3.147	2531	15.7	41.0	1.461	0.592
	4102	18.3	40.0	1.530	2.647	4.072	0.965	2.891	1370	25.9	46.0	0.950	1.719
	4610	24.0	39.0	1.110	−0.766	3.413	0.999	6.305	4600	24.0	39.0	1.040	1.155
	4101	16.3	41.6	1.500	2.780	4.344	0.976	2.759	2530	22.6	45.0	1.361	0.638
									4620	24.0	39.0	1.210	1.397
									3190	16.5	47.9	1.410	0.657
Average					2.647	4.258	0.972	2.892					0.996
Clay	4681	11.6	54.4	1.080	−0.226	3.625	0.969	5.765	2361	3.5	57.0	1.387	0.516
	4121	7.2	53.2	1.110	−1.203	3.227	0.997	6.742	1400	4.7	58.0	1.450	0.487
	2360	20.5	45.0	1.420	−0.262	3.531	0.986	5.801	4680	13.8	47.3	1.100	1.065
									4120	11.8	50.8	1.240	0.549
									2362	3.8	63.0	1.250	0.542
Average					−0.488	3.506	0.976	6.027					0.670
Average for all textures					0.482	3.602	0.938	5.507					0.878

† UNSODA code.
‡ Bulk density.

for effective saturation, and then dividing the sum by the bulk volume of the sample, given by $(1/\rho_b)$. Pore volume associated with each particle-size fraction equals $(w_i/\rho_p)e$. Combining these terms and simplifying yields Eq. [2], which gives θi in terms of mass fraction, w_i, effective saturation, S_w, and porosity, ϕ.

Equation [5] is used to compute flow rate for a single pore, q_i, in each pore-size fraction with c and x given in Table 3. As discussed above, estimates of c and x can be obtained using Eq. [16] through Eq. [19]. The number of pores, in each pore-size fraction, N_{pi}, is calculated using Eq. [11], [12], and [13]. Pore flow for a single pore is multiplied by N_{pi} to obtain the flow rate, Q_i, for the ith pore-size fraction (Eq. [3]). A summation of Q_i from fraction $j = 1$ to i yields the flow rate for the sample corresponding with θ_i. Since all flow rates correspond with a unit gradient, dividing $\Sigma_{j=1}^{j=i} Q_j$ by the bulk cross-sectional area of the sample, A_b, gives the hydraulic conductivity, $K(\theta_i)$ (Eq. [15]).

RESULTS AND DISCUSSION

Pore Flow in Idealized Capillary Tubes and Soil Pores

Figure 1 shows an example of the relationship between the logarithm of the pore flow rate, q_i and log r_i for 16 soils, representing sand, sandy loam, loam, and clay textures. The Hagen-Poiseuille pore flow rates were based on Eq. [4], assuming that pores are circular and straight capillary tubes. The experimental pore flow rates were calculated from measured $K(\theta)$ data using Eq. [16], [17], and [18]. Similar plots for individual textural classes showed a strong linear relationship between logq_i and logr_i (see parameters and r^2 values in Table 3). We conclude that a linear relationship between logq_i and logr_i holds not only for the straight capillary tubes, but also for tortuous porous materials. The difference between the two is indicated by the slopes and intercepts of the regression lines (see Table 3). In the case of the

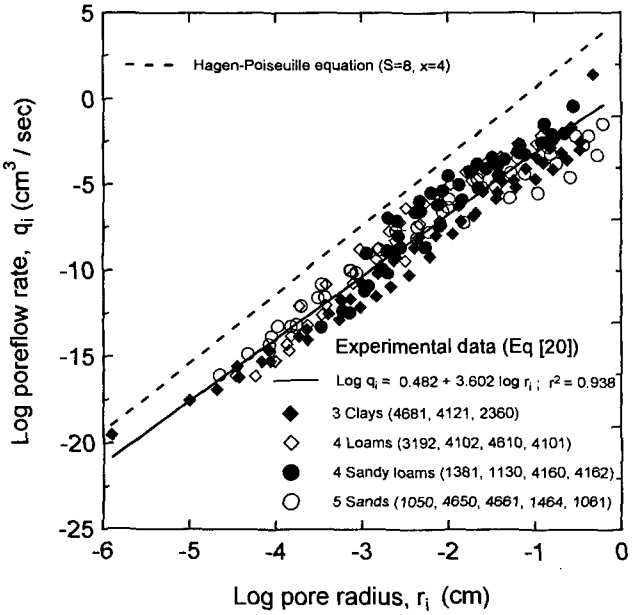

Fig. 1. Relationship between pore flow rate and pore radii for 16 soils, representing sand, sandy loam, loam, and clay textures.

Hagen-Poiseuille equation, $x = 4$, $S = 8$, $\eta = 0.008904$ poise (25°C), and $g = 980$ cm s^{-2}. For the soil samples, the value of x is equal to the coefficient of regression and S can be calculated from log$c$ = log$(\pi\rho_w g/S\eta)$. For our calculations, we assumed the viscosity of water at 25°C to be applicable to all samples, since all experimental data were obtained at room temperature. The calculated values of log c, x, and S for four textural classes are summarized in Table 3. Results show that x varies from ≈2.66 to ≈4.71. Values of S, on the other hand, are quite large and vary within and between textural classes by orders of magnitude.

The deviations in x and S of the soils from those for a bundle of straight and circular capillary tubes reflect the combined effects of pore size, pore-size distribution, pore shape, tortuosity, interaction between pores, viscosity of water, and possibly other factors. The values of x and S (Table 3) in our analysis represent only the gross properties of soil materials. It is quite possible that they both vary with pore size in a given sample. The lack of a systematic trend in x and S with textural class is not surprising. Soils within a textural class represent wide variations in PSD, bulk density, and organic matter content. Our grouping of x and S by textural class is only for convenience. Further investigation of the behavior of x and S is beyond the scope of this initial model of $K(\theta)$ based on the PSD. However, results in Fig. 1 demonstrate that the model for flow in straight capillary tubes can be modified to adequately describe the macroscopic flow behavior in porous media.

Predicted Hydraulic Conductivity Functions

The empirically estimated values of c and x were used in Eq. [5] to independently calculate hydraulic conductivity functions, $K(\theta)$, of 16 soils. These soils are identified in Table 3. Examples of predicted and experimental data are presented in Fig. 2a (sand), 2b (loam), and 2c (clay). Overall, the shapes of the predicted $K(\theta)$ functions were similar to those of the measured data in the range of wetness for which measured data were available. However, quantitative agreements between predicted and experimental values varied, partly because the majority of the experimental data sets were limited to a relatively narrow range of water contents (usually in the wet range). The model, on the other hand, predicted hydraulic conductivity values across a wide range of water contents — from near saturation to extreme dryness. However, because of a lack of measured data in the dry range, model predictions cannot be validated.

Figure 3 shows a comparison of the logarithms of experimental vs. predicted hydraulic conductivity values for all soils on a 1:1 scale. The regression line between the experimental and predicted $K(\theta)$ values closely matches the 1:1 line with an r^2 of 0.807. The RMSRs of the log-transformed predicted and experimental $K(\theta)$ data ranged from 0.616 to 1.603 for sand (average 1.000), from 0.592 to 1.719 for loam (average 0.996), and from 0.487 to 1.065 for clay (average 0.670). The average RMSR for all textures was 0.878. Similar RMSR values

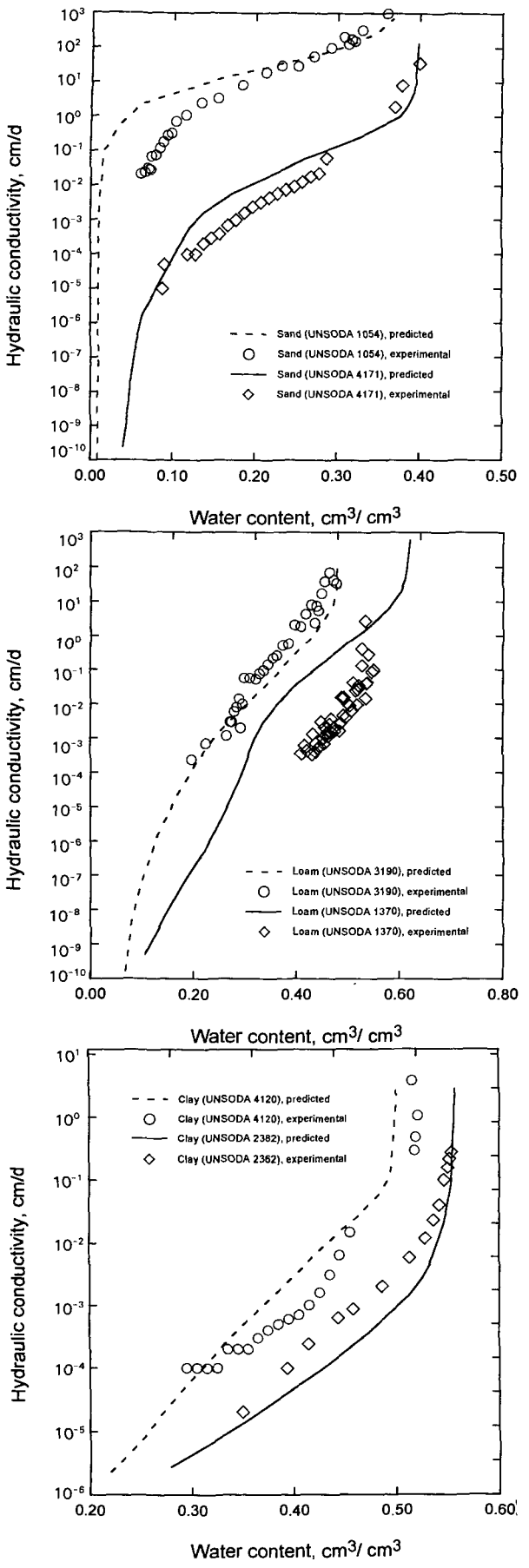

Fig. 2. Comparison of predicted and experimental hydraulic conductivity functions: (a) sand, (b) loam, and (c) clay.

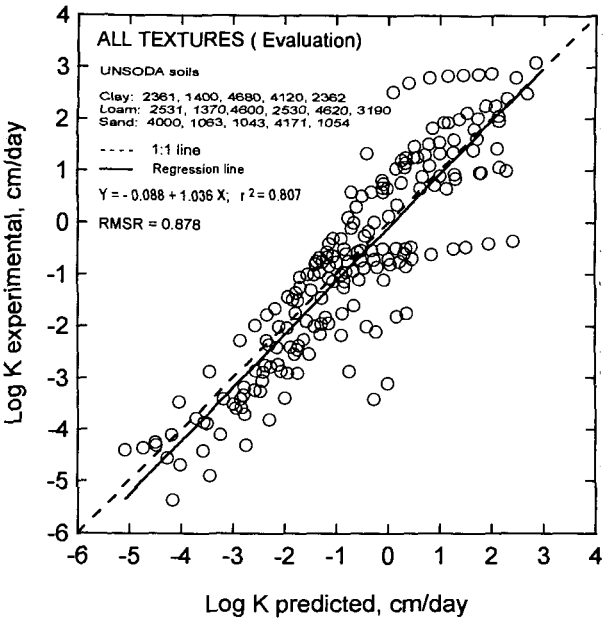

Fig. 3. Comparison of predicted and experimental hydraulic conductivity. Test results for 16 soils are pooled.

have been observed with other hydraulic conductivity prediction models (e.g., Schaap and Leij, 1998). The scatter in the data is not surprising in view of the many sources of variation in the experimental as well as input data. Measurement of hydraulic conductivity is usually difficult, and large differences in experimentally measured hydraulic conductivity between replicated samples of the same soil are not uncommon (e.g., Dirksen, 1991). There are many examples in the literature showing such variations, as well as large variations between measurements and prediction models (e.g., El-Kadi, 1985; Mishra and Parker, 1992; Yates et al., 1992; Tamari et al., 1996; Poulsen et al., 1998). These variations may be attributed to differences in PSD, bulk density, mineralogy, microaggregation, and organic matter content within a textural class. We used textural class average values of the model parameters, c and x. However, it should be noted that textural similarities do not necessarily translate into hydrophysical similarities. Grouping soils together solely on the basis of textural nomenclature may introduce variations of up to 25 percentage points in the mass fraction of some particle-size ranges (L.M. Arya, 1983, unpublished data, based on USDA-SCS [1974]). Significant variations in bulk density and organic matter content also exist within a textural class. Variations in experimental procedures and associated errors may introduce additional noise in the experimental data. Hydraulic properties of soils in the UNSODA database (Leij et al., 1996) are heterogenous and exhibit large within-texture variations (see Fig. 2, for example). These data were contributed by researchers in the USA, Netherlands, United Kingdom, Germany, Belgium, Denmark, Russia, Italy, Japan, and Australia, who used different experimental procedures. In view of the above

uncertainties, we believe that the predictions of the proposed PSD-based model of the hydraulic conductivity are quite reasonable. Predictions of the model may be further improved if measurable physical characteristics of soils that influence flow processes can be identified.

SUMMARY AND CONCLUSIONS

Research reported here describes a method to compute the hydraulic conductivity function from the PSD and bulk density data. The pore-size distribution is based on the Arya-Paris model (1981) as modified by Arya et al. (1999). The pore flow rate is related to pore radii in a manner similar to that for idealized capillary tubes, described by the Hagen-Poiseuille equation. However, the model parameters for flow in natural soil are determined empirically. They deviate significantly from those for the idealized model, and reflect the effects of pore size, shape, and other unknown factors. The effects of packing density and pore tortuosity are incorporated by the scaling parameter, α, of the Arya-Paris model. The model predicts hydraulic conductivity function across a wide range of water contents, from near saturation to extreme dryness. Unlike other models, the need for a measured soil water retention function is eliminated because the pore-size distribution is derived directly from the PSD. Likewise, the need for a measured saturated hydraulic conductivity as a matching point is also eliminated. Our flow model requires only two parameters of concern: c and x. The behavior of these parameters may be further elucidated as the model is subjected to further tests and scrutiny.

Predictions of the hydraulic conductivity for a number of soils, representing a range in texture, bulk density, and organic matter content were reasonable. The RMSEs of log-transformed predicted and experimental data ranged from a low of 0.487 to a high of 1.562, the averaged being 0.878. Heterogeneity in experimental data and nonconformity between gross textural class attributes and hydrophysical behavior of individual soils are believed to be responsible for uncertainties in the model's predictions.

REFERENCES

Arya, L.M., and J.F. Paris. 1981. A physicoempirical model to predict soil moisture characteristics from particle-size distribution and bulk density data. Soil Sci. Soc. Am. J. 45:1023–1030.

Arya, L.M., F.J. Leij, M.Th. van Genuchten, and P.J. Shouse. 1999. Scaling parameter to predict the soil water characteristic from particle-size distribution data. Soil Sci. Soc. Am. J. 63:510–519.

Batchelor, G.K. 1967. An introduction to fluid dynamics. Cambridge Univ. Press, Cambridge, UK.

Bouma, J., and J.A.J. van Lanen. 1987. Transfer functions and threshold values: from soil to land qualities. p. 106–110. *In* K.J. Beek et al. (ed.) Quantified land evaluation. International Institute Aerospace Surv. Earth Sci. ITC Publ. 6:106–110.

Childs, E.C. 1969. The physical basis of soil water phenomena. John Wiley and Sons, New York.

Childs, E.C., and N. Collis-George. 1950. The permeability of porous materials. Proc. R. Soc. Ser. A. 201:392–405.

Corey, A.T. 1992. Pore-size distribution. p. 37–44. *In* M.Th. van Genuchten et al. (ed.) Proc. Int. Workshop on Indirect Methods of Estimating the Hydraulic Properties of Unsaturated Soils. 11–13 Oct. 1989. U.S. Salinity Laboratory and Dep. Soil and Envir. Sci., Univ. of California, Riverside.

Dirksen, C. 1991. Unsaturated hydraulic conductivity. p. 209–269. *In* K. Smith and C. Mullins (ed.) Soil analysis: Physical methods. Marcel Dekker, New York.

Eching, S.O., J.W. Hopmans, and O. Wendroth. 1994. Unsaturated hydraulic conductivity from transient multistep outflow and soil water pressure data. Soil Sci. Soc. Am. J. 58:687–695.

El-Kadi, A.I. 1985. On estimating the hydraulic properties of soil. II. A new empirical equation for estimating hydraulic conductivity for sands. Adv. Water Resour. 8:148–153.

Garnier, P., M. Rieu, P. Boivin, M. Vauclin, and P. Beveye. 1997. Determining the hydraulic properties of a swelling soil from a transient evaporation experiment. Soil Sci. Soc. Am. J. 61:1555–1563.

Green, R.E., L.R. Ahuja, and S.K. Chong. 1986. Hydraulic conductivity, diffusivity, and sorptivity of unsaturated soils: field methods. p. 771–798. *In* A. Klute (ed.) Methods of soil analysis. Part 1. Agron. Monogr. 9. ASA and SSSA, Madison, WI.

Hillel, D. 1971. Soil and water: Physical principles and processes. Academic Press, New York.

Klute, A., and C. Dirksen. 1986. Hydraulic conductivity and diffusivity: Laboratory methods. p. 687–734. *In* A. Klute (ed.) Methods of soil analysis. Part 1. Agron. Monogr. 9. ASA and SSSA, Madison, WI.

Leij, F.J., W.J. Alves, M.Th. van Genuchten, and J.R. Williams. 1996. Unsaturated soil hydraulic database, UNSODA 1.0 user's manual. Report EPA/600/R-96/095. U.S. EPA, Ada, OK.

Marshall, T.J. 1958. A relation between permeability and size distribution of pores. J. Soil Sci. 9:1–8.

Mishra, S., J.C. Parker, and N. Singhal. 1989. Estimation of soil hydraulic properties and their uncertainty from particle-size distribution data. J. Hydrol. 108:1–18.

Mualem, Y. 1976. A new model for predicting the hydraulic conductivity of unsaturated porous media. Water Resour. Res. 12:513–522.

Mualem, Y. 1992. Modeling the hydraulic conductivity of unsaturated porous media. p. 15–36. *In* M.Th. van Genuchten et al. (ed.) Proc. Int. Workshop on Indirect Methods of Estimating the Hydraulic Properties of Unsaturated Soils. 11–13 Oct. 1989. U.S. Salinity Laboratory and Dep. Soil and Envir. Sci., Univ. of California, Riverside.

Mualem, Y., and G. Dagan. 1978. Hydraulic conductivity of soils: unified approach to the statistical models. Soil Sci. Soc. Am. J. 42:392–395.

Poulsen, T.G., P. Moldrup, and O.H. Jacobsen. 1998. One-parameter models for unsaturated hydraulic conductivity. Soil Sci. 163: 425–435.

Rieu, M., and G. Sposito. 1991. Fractal fragmentation, soil porosity, and water properties: I. Theory. Soil Sci. Soc. Am. J. 55:1231–1238.

Schaap, M.G., and F.J. Leij. 1998. Using neural networks to predict soil water retention and soil hydraulic conductivity. Soil Tillage Res. 47:37–42.

Schuh, W.M., and J.W. Bauder. 1986. Effect of soil properties on hydraulic conductivity-moisture relationships. Soil Sci. Soc. Am. J. 50:848–855.

Schuh, W.M., and R.L. Cline. 1990. Effect of soil properties on unsaturated conductivity pore-interaction factors. Soil Sci. Soc. Am. J. 54:1509–1519.

Smettem, K.J.J., and B.E. Clothier. 1989. Measuring unsaturated sorptivity and hydraulic conductivity using multiple disc permeameters. J. Soil Sci. 40:563–568.

Tamari, S., H.M. Wosten, and J.C. Ruiz-Suarez. 1996. Testing an artificial neural network for predicting soil hydraulic conductivity. Soil Sci. Soc. Am. J. 60:1732–1741.

Tyler, S.W., and S.W. Wheatcraft. 1988. Application of fractal mathematics to soil water retention estimation. Soil Sci. Soc. Am. J. 53:987–996.

USDA-SCS. 1974. Soil survey laboratory data and descriptions for some soils of New Jersey. Report no. 26. New Jersey Agricultural Experiment Station, Rutgers Univ.

van Genuchten, M.Th. 1980. A closed-form equation for predicting the hydraulic conductivity of unsaturated soils. Soil Sci. Soc. Am. J. 44:892–898.

van Genuchten, M.Th., and F. Leij. 1992. On estimating the hydraulic properties of unsaturated soils. p. 1–14. *In* M.Th. van Genuchten

et al. (ed.) Proc. Int. Workshop on Indirect Methods of Estimating the Hydraulic Properties of Unsaturated Soils. 11–13 Oct. 1989. U.S. Salinity Laboratory and Dep. Soil and Envir. Sci., Univ. of California, Riverside.

Vereecken, H. 1995. Estimating the unsaturated hydraulic conductivity from theoretical models using simple soil properties. Geoderma 65:81–92.

Vereecken, H., J. Maes, and J. Feyen. 1990. Estimating unsaturated hydraulic conductivity from easily measured soil properties. Soil Sci. 149:1–12.

Wildenschild, D., K.H. Jensen, K.J. Hollenbeck, T.H. Illangasekare, D. Znidarcic, T. Sonnenborg, and M.B. Butts. 1997. A two-stage procedure for determining unsaturated hydraulic characteristics using syringe pump and outflow observations. Soil Sci. Soc. Am. J. 61:347–359.

Wösten, J.H.M., and M.Th. van Genuchten. 1988. Using texture and other soil properties to predict the unsaturated soil hydraulic functions. Soil Sci. Soc. Am. J. 52:1762–1770.

Yates, S.R., M.Th. van Genuchten, and F.J. Leij. 1992. Analysis of predicted hydraulic conductivities using RETC. p. 273–283. *In* M.Th. van Genuchten et al. (ed.) Proc. Int. Workshop on Indirect Methods of Estimating the Hydraulic Properties of Unsaturated Soils. 11–13 Oct. 1989. U.S. Salinity Laboratory and Dep. Soil and Envir. Sci., Univ. of California, Riverside.